Three-body forces between charged colloidal particles

C. Russ and H. H. von Grünberg
Fakultät für Physik, Universität Konstanz, 78457 Konstanz, Germany

M. Dijkstra
Debye Institute, Soft Condensed Matter Physics, Utrecht University, Princetonplein 5, 3584 CC Utrecht, The Netherlands

R. van Roij
Institute for Theoretical Physics, Utrecht University, Leuvenlaan 4, 3584 CE Utrecht, The Netherlands

(Received 19 March 2002; published 15 July 2002)

Within nonlinear Poisson-Boltzmann theory we calculate the pair and triplet interactions between charged colloidal spheres, specifically in the nonlinear regime of low salt concentrations and high charges. We find repulsive pair interactions and attractive triplet interactions. Within a van der Waals-like mean-field theory we estimate in which parameter regime a gas-liquid coexistence is to be expected.

DOI: 10.1103/PhysRevE.66.011402 PACS number(s): 82.70.Dd, 64.60.Cn, 64.10.+h

I. INTRODUCTION

Suspensions of charge-stabilized colloidal particles have long been understood in terms of the DLVO (Derjaguin, Landau, Verwey, and Overbeek) theory [1]. This theory predicts that the effective interactions between a pair of charged colloids immersed in a simple electrolyte consist of the sum of (i) hard-core repulsions due to the finite diameter σ of the colloidal spheres, (ii) van der Waals attractions with a typical range of a few nm from the colloidal surface, and (iii) screened-Coulomb (Yukawa) repulsions with the screening length given by the Debye length κ^{-1} of the electrolyte. The relative strengths of these contributions can be varied by changing the solvent, salt concentration, or temperature. For instance, by increasing the salt concentration the electrostatic screening becomes more efficient (κ^{-1} decreases), hence the van der Waals attractions become relatively more pronounced, and this explains reversible vapor-liquid coexistence or irreversible flocculation if the salt concentration is high enough [2]. Conversely, by decreasing the salt concentration the screened-Coulomb repulsions act on longer distances (κ^{-1} increases), thereby stabilizing the suspension by masking the van der Waals attractions, which explains, e.g., a first-order fluid-to-crystal transition upon increasing the colloidal density and the existence of colloidal crystals at colloid volume fractions of only a few percent [3]. For these reasons, and many more, the DLVO theory has long been considered a cornerstone of colloid science.

During the past few years, however, evidence has been accumulating that the DLVO picture breaks down, or at least needs refinement, in the regime of extremely low-salt concentrations below, say, a few micromoles per liter. For water at room-temperature this regime is such that κ^{-1} is of the order of 100 nm or larger, i.e., the electrostatic repulsions should mask the van der Waals attractions completely according to the DLVO theory. Nevertheless, some experiments provide evidence for the existence of attractive interactions between the colloids in this regime. The experimental observations include vapor bubbles (''voids'') in otherwise homogeneous suspensions [4], lattice spacings of colloidal crystals smaller than expected on the basis of the total density (suggesting gas-solid coexistence) [5], long-lived metastable crystallites [6], and gas-liquid coexistence [7] (albeit a disputed one [8]). Even though the experimental situation is far from clear, these results did trigger a search for the source of possible attractive electrostatic interactions between like-charged colloids. Several papers review the current state-of-affairs comprehensively, see, e.g., Refs. [9–11].

By now several mechanisms have been identified and proposed. One can distinguish between approaches aiming at improving the DLVO pair interactions by, e.g., including ionic correlations, and those where many-body effects are considered. It has become clear that ion-ion correlations and correlated fluctuations can indeed give rise to an attractive component in the effective pair interactions [12–18], and so can the Coulombic depletion effect [19]. It remains to be seen, however, whether these attractions are strong enough and of sufficiently long range to explain the experimental low-salt data. Moreover, in the process of extracting thermodynamic and structural information of a suspension from pair interactions, one tacitly assumes pairwise additivity. In the low-salt regime of interest, where κ^{-1} is of the order of σ or even larger, it is rather likely that pairwise additivity breaks down and that many-body effects become important. These many-body effects have been included through so-called volume terms [20–24], which are coordinate-independent but density-dependent contributions to the effective Hamiltonian of the colloids. The nontrivial density-dependence of the volume term can be traced back to a ''smearing'' effect, where (parts of) the coordinate dependences of the effective pair and many-body interactions are ''projected'' onto effective, density-dependent one- and two-body terms in the effective Hamiltonian. This smearing occurs by, e.g., linearizing the Poisson-Boltzmann equation about the average potential or the average ion concentration instead of solving the full nonlinear problem [25]. Given the manifestly attractive (cohesive) contributions to the volume term, at low enough salt, we expect attractive many-body interactions within a full nonlinear theory for the effective colloidal interactions. This would also be consistent with recent simulation work in

Refs. [26,27]. In this paper we study the pair and triplet interactions between charged colloids within the framework of Poisson-Boltzmann theory, i.e., within mean-field theory. Given the low-salt conditions of interest, we ignore the van der Waals interactions from the outset, and only consider Coulombic and hard-core interactions.

This study was motivated by a pilot study by one of us, where the pair, triplet, and four-body interactions of infinite, parallel, highly charged plates were calculated within Poisson-Boltzmann theory [28]. The result was that the pair interactions are purely repulsive, as expected. The triplet interactions, however, were found to be attractive, and such that the pair interaction between the two outer plates was canceled exactly (within the numerical accuracy) by the triplet interaction. This implies that the middle plate completely shields the outer two plates from each other, i.e., one could interpret this as an instance of screening by a macroion. The four-body interaction is found to be repulsive again, in such a way that the effective Hamiltonian of a system of four parallel charged plates is a sum over nearest-neighbor pair interactions—this is very different from a sum over all pairs. The question we address in this paper is whether these phenomena for parallel plates have any resemblance to the physical reality of charged spheres.

This article is organized as follows. In Sec. II we show how the effective pair, triplet, and more-body potentials between charged colloids follow from the solution of the Poisson-Boltzmann equation. In Sec. III we discuss the implementation of the numerical scheme and the results for the pair and triplet potentials. In Sec. IV we estimate, on the basis of a simple van der Waals-like theory, whether the attractive triplet interactions are strong enough to stabilize a dense liquid in coexistence with a dilute gas. We conclude in Sec. V.

II. POISSON-BOLTZMANN THEORY

We consider N identical colloidal particles at center-of-mass coordinates $\mathbf{r}_i$ $(i=1,\ldots,N)$ immersed in an unbounded 1:1 electrolyte solution. The colloids are assumed to be spherical, with hard-core diameter σ, and negatively charged, with the total charge $-Ze$ distributed homogeneously on the colloidal surface. Here e represents the unit (proton) charge. The electrolyte, at temperature T, is characterized by the dielectric constant ϵ of the solvent (which we treat as a structureless continuum), and by the bulk salt concentration c_s of positive and negative ions, i.e., the total bulk ion concentration is $2c_s$. For later reference we introduce the Bjerrum length $\lambda_B=e^2\beta/\epsilon$, with $\beta=1/kT$. It turns out to be convenient to divide space into regions inside and outside the hard core of the colloids. The region of space filled by the electrolyte solution, i.e., outside the colloids, is denoted by G, and the boundaries of this region, which are the surfaces of the N colloidal particles $(i=1,\ldots,N)$, are denoted by ∂G_i. Our first goal is to compute the average electrostatic potential, $\psi(\mathbf{r})=\psi(\mathbf{r};\{\mathbf{r}_i\})$, for fixed colloid configurations $\{\mathbf{r}_i\}$, for $\mathbf{r}\in G$.

Due to the presence of the (fixed) colloidal charges, the distribution of microions becomes inhomogeneous near the colloids. In a mean-field approach, the density distributions of the positive and negative ions, $\rho_\pm(\mathbf{r})$, are related to $\psi(\mathbf{r})$ through the Boltzmann distribution $\rho_\pm(\mathbf{r})=c_s\exp[\mp\Phi(\mathbf{r})]$ for $\mathbf{r}\in G$, where $\Phi(\mathbf{r})=\beta e\psi(\mathbf{r})$ is the dimensionless electrostatic potential. The ionic charge distribution is therefore, for $\mathbf{r}\in G$, given by

$$\rho(\mathbf{r})=\rho_+(\mathbf{r})-\rho_-(\mathbf{r})=-2c_s\sinh\Phi(\mathbf{r}). \tag{1}$$

Outside G we have $\rho(\mathbf{r})=0$ from the hard-core condition. The two unknown fields $\rho(\mathbf{r})$ and $\Phi(\mathbf{r})$ also satisfy the Poisson equation $\nabla^2\Phi(\mathbf{r})=-4\pi\lambda_B\rho(\mathbf{r})$, which yields with Eq. (1), the Poisson-Boltzmann (PB) equation

$$\nabla^2\Phi(\mathbf{r})=\kappa^2\sinh\Phi(\mathbf{r}),\quad \mathbf{r}\in G, \tag{2}$$

where the screening parameter κ is defined as $\kappa^2=8\pi\lambda_B c_s$. The PB equation is a nonlinear partial differential equation for $\Phi(\mathbf{r})$, to be solved with the boundary conditions (BCs) that

$$\Phi(\mathbf{r})=0,\quad |\mathbf{r}|\to\infty; \tag{3}$$

$$\mathbf{n}_i\cdot\nabla\Phi(\mathbf{r})=\frac{4\pi\lambda_B Z}{\pi\sigma^2},\quad \mathbf{r}\in\partial G_i,$$

where $\mathbf{n}_i$ are unit vectors, normal to the surfaces ∂G_i of the colloids labeled $i=1,\ldots,N$, and pointing into the region G. Note that the last line of Eq. (3) is the constant-charge boundary condition. Due to the negative colloidal charges, Φ is negative in G with a positive gradient at ∂G_i in the direction of G. The BCs of Eq. (3) are such that (i) the bulk ion concentrations $\rho_\pm(\mathbf{r})\to c_s$ far from the colloidal particles, and (ii) the total system is charge neutral. This latter point follows from the spatial integration of $\rho(\mathbf{r})$ over G, which with Eqs. (1) and (2) and a partial integration yields NZ as required.

The potential $\Phi(\mathbf{r})$ is the key to the calculation of the effective interactions of the colloids. Describing the electrolyte in the grand-canonical ensemble, i.e., fixing the volume, the temperature T, and the chemical potential of the microions $\mu_s=kT\ln c_s\Lambda^3$ (with Λ^3 the thermal wave length), we can describe the effective interactions as the grand potential of the electrolyte in the external field of the N fixed colloidal particles. In terms of $\Phi(\mathbf{r})$ and the densities $\rho_\pm(\mathbf{r})$, the grand potential Ω is, within mean-field theory, given by the sum of the electrostatic energy and the ideal-gas grand potential, viz.,

$$\beta\Omega=\frac{1}{8\pi\lambda_B}\int_G d\mathbf{r}(\nabla\Phi)^2+\sum_{\alpha=\pm}\int_G d\mathbf{r}\rho_\alpha(\ln\rho_\alpha\Lambda^3-1-\beta\mu_s)+2\int_G d\mathbf{r}c_s. \tag{4}$$

Note that we subtracted the grand potential of the uncharged system through the last term of Eq. (4). This expression for Ω follows directly from the optimization of the mean-field

grand potential functional with respect to $\rho_{\pm}(\mathbf{r})$, see, e.g., Ref. [25]. By substitution of $\rho_{\pm}=c_s\exp[\mp\Phi]$, Eq. (4) can be further simplified to

$$\beta\Omega=\frac{1}{8\pi\lambda_B}\int_G d\mathbf{r}[(\boldsymbol{\nabla}\Phi)^2+2\kappa^2(\Phi\sinh\Phi-\cosh\Phi+1)]$$
$$=-\frac{Z}{2\pi\sigma^2}\sum_{i=1}^{N}\int_{\partial G_i}d\mathbf{r}\Phi+\frac{\kappa^2}{8\pi\lambda_B}\int_G d\mathbf{r}(\Phi\sinh\Phi$$
$$-2\cosh\Phi+2). \tag{5}$$

Note that Ω vanishes in the case of uncharged colloids, where $\Phi\equiv 0$. Once we have calculated $\Phi(\mathbf{r})$ for a given configuration of colloidal particles by solving the PB problem represented by the Eqs. (2) and (3), we can evaluate Eq. (5) to obtain Ω. A change of the position of any of the colloidal particles changes $\Phi(\mathbf{r})$ and, hence, $\beta\Omega$. This change of Ω can be related to the effective interactions between the colloids, as we will see now.

For a system of N colloidal particles, at fixed positions $\mathbf{r}_i$, $i=1,\ldots,N$, we denote the grand potential, given by Eq. (5), by Ω_N from now on. This quantity, which is a function of the coordinates $\mathbf{r}_i$, can be uniquely decomposed into so-called effective n-body potentials $\Omega^{(n)}$, with $n\leqslant N$, viz.,

$$\Omega_N=N\Omega_1+\sum_{i<j}^{N}\Omega^{(2)}(ij)+\sum_{i<j<k}^{N}\Omega^{(3)}(ijk)$$
$$+\sum_{i<j<k<l}^{N}\Omega^{(4)}(ijkl)+\cdots, \tag{6}$$

where the short-hand notation for the center-of-mass positions should be obvious, and where $\cdots$ denotes five-body potentials and higher. The n-body potential is defined in the n-body system, i.e., in the system with $N=n$. The decomposition scheme starts by subsequently considering the cases $N=1,2,3,\ldots$. Clearly Ω_1 is the self-energy of a single colloid, $N=1$, in the ''grand-canonical sea'' of electrolyte. It is an intensive quantity, which does not depend on the center-of-mass position $\mathbf{r}_1$ of that colloid by translational invariance. The effective pair potential $\Omega^{(2)}(r_{12})\equiv\Omega^{(2)}(12)$ between two colloids at separation $r_{12}=|\mathbf{r}_1-\mathbf{r}_2|$ follows from Eq. (6), for the case $N=2$, as

$$\Omega^{(2)}(12)=\Omega_2(12)-2\Omega_1. \tag{7}$$

Note that $\Omega^{(2)}(r_{12})$ tends to zero for $r_{12}\to\infty$ by construction. The three-body potential $\Omega^{(3)}(r_{12},r_{13},r_{23})=\Omega^{(3)}(123)$ is defined in the $N=3$ system as

$$\Omega^{(3)}(123)=\Omega_3(123)-\Omega^{(2)}(12)-\Omega^{(2)}(13)$$
$$-\Omega^{(2)}(23)-3\Omega_1. \tag{8}$$

By construction, $\Omega^{(3)}(123)$ tends to zero whenever (at least) one of the arguments $r_{ij}\to\infty$.

It is straightforward to proceed and define the four-body potential by equating the left- and right-hand side of Eq. (6) for $N=4$, etc. In this sense the decomposition scheme presented here is nothing but a scheme of subsequent definitions, producing merely an identity. The power of the scheme lies, however, in its low-order truncation; whereas a real suspension consists of many colloids, say $N=10^{12}$ or so, one expects that the decomposition of Ω_N of Eq. (6) is accurate by only including n-body potentials of order $n=2,\ldots,n^*$, with n^* of order unity, i.e., by assuming that $\Omega^{(n)}\equiv 0$ for $n>n^*$. In fact, in many cases one just restricts attention to $n^*=2$ only, ignoring even 3-body interactions. This assumption of pairwise additivity is for instance made when describing the Hamiltonian of noble gases by a sum of Lennard-Jones potentials, or the effective Hamiltonian of a colloidal suspension by pairwise DLVO interactions. The focus of this article is on the case $n^*=3$, the lowest-order correction to pairwise additivity.

We close this section with a reduction in the number of independent parameters by an appropriate scaling to dimensionless variables. We use the hard-sphere diameter σ as unit of length, and define the dimensionless gradient operator $\overline{\boldsymbol{\nabla}}=\sigma\boldsymbol{\nabla}$ and the dimensionless screening parameter $\overline{\kappa}=\kappa\sigma$. In terms of these, the Poisson-Boltzmann problem can be rewritten as

$$\overline{\nabla}^2\Phi(\mathbf{r})=\overline{\kappa}^2\sinh\Phi(\mathbf{r}),\quad \mathbf{r}\in G, \tag{9}$$
$$\mathbf{n}_i\cdot\overline{\boldsymbol{\nabla}}\Phi(\mathbf{r})=4\overline{Z},\quad \mathbf{r}\in\partial G_i,$$

where the rescaled (and dimensionless) colloidal charge is defined as $\overline{Z}=Z\lambda_B/\sigma$. The rescaled grand potential is defined as $\overline{\Omega}_N=\beta\Omega_N\lambda_B/\sigma$, and is given by

$$\overline{\Omega}_N=-\frac{\overline{Z}}{2\pi}\sum_{i=1}^{N}\int_{\partial G_i}d\mathbf{r}\Phi+\frac{\overline{\kappa}^2}{8\pi}\int_G d\mathbf{r}(\Phi\sinh\Phi$$
$$-2\cosh\Phi+2), \tag{10}$$

where the spatial coordinates are understood to be in units of σ. One recognizes that the problem depends on just two independent parameters: the scaled screening length $\overline{\kappa}^{-1}$ and the scaled charge $\overline{Z}$. Systematically varying these two parameters, each time calculating the effective potentials $\overline{\Omega}^{(n)}=\beta\Omega^{(n)}\lambda_B/\sigma$ from the generalized grand potential $\overline{\Omega}_N$, we can conveniently explore the behavior of a whole variety of possible systems, each characterized by the parameter set $(\lambda_B,\ \sigma,\ \kappa,\ Z)$. It is important to realize, however, that this reduction to only two dimensionless parameters only applies to the calculation of the effective interactions; the thermodynamics of the suspension is determined by $\beta\Omega$ rather than by $\overline{\Omega}$, and hence the ratio λ_B/σ is, in this respect, another independent dimensionless combination. Note that typical colloidal parameters are $\lambda_B\simeq 1$ nm, $Z\simeq 100$–1000, $\sigma\simeq 100$ nm, and $\kappa^{-1}\simeq 1$–1000 nm, such that typically $\overline{Z}\simeq 1$–10, $\overline{\kappa}\simeq 0.01$–$10$, and $\lambda_B/\sigma\simeq 0.01$. The combinations of

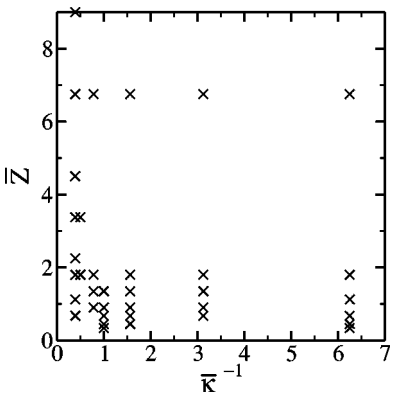

FIG. 1. Points in the parameter space $(\bar{\kappa}^{-1},\bar{Z})$ investigated in this work. Here $\bar{\kappa}=\kappa\sigma$ is the dimensionless screening constant κ, $\bar{Z}=Z\lambda_B/\sigma$ the dimensionless colloidal charge Z, and σ and λ_B are the colloidal diameter and the Bjerrum length, respectively.

$\bar{\kappa}$ and $\bar{Z}$ investigated in this work are illustrated in Fig. 1. They are seen to span a large regime of typical colloidal parameters.

III. THREE-BODY INTERACTIONS

A. General remarks

The decomposition of Eq. (6), truncated such that $\Omega^{(n)}$ is assumed to vanish for $n>n^*$, is in fact a construction with which an N-body system (with $N\gg 1$) can be approximately described by a series of 1,2, . . . ,n^*-body systems, with n^* of order unity. The focus of this article is on the case $n^*=3$, i.e., we restrict explicit computations to systems consisting of $N=1,2,3$ colloidal particles. Before discussing the details of our numerical calculations, we wish to stress that many-body potentials are, essentially, a feature of the nonlinear character of the Poisson-Boltzmann equation. In the linear PB theory—where conventionally $\sinh\Phi\simeq\Phi$ in Eq. (2)—the linear superposition principle applies, and this yields, essentially, vanishing many-body interactions. This can be easily seen from the following consideration. In linear PB theory, the expression in Eq. (10) for the grand potential must be expanded up to second order. This yields

$$\bar{\Omega}_{lin}=-\frac{\bar{Z}}{2\pi}\sum_{i=1}^{N}\int_{\partial G_i}d\mathbf{r}\Phi. \tag{11}$$

Since the PB equation is now linear, Φ is approximately given by a multicentered sum, i.e., a superposition, of N potentials $\varphi_j\equiv\varphi(\mathbf{r}-\mathbf{r}_j)$, i.e., $\Phi\simeq\Sigma_{j=1}^{N}\varphi_j$, where φ_j is calculated for a single, isolated colloidal particle. As a consequence

$$\bar{\Omega}_{lin}=-\frac{\bar{Z}}{2\pi}\sum_{i,j=1}^{N}\int_{\partial G_i}d\mathbf{r}\varphi_j\equiv N\bar{\Omega}_{1,lin}+\sum_{i<j}^{N}\bar{\Omega}^{(2)}_{lin}(ij), \tag{12}$$

where the linearized one-body term (self-energy) $\bar{\Omega}_{1,lin}$ and the effective pair potential $\bar{\Omega}^{(2)}_{lin}(ij)$ are given by

$$\bar{\Omega}_{1,lin}=-\frac{\bar{Z}}{2\pi}\int_{\partial G_i}d\mathbf{r}\varphi_i,$$

$$\bar{\Omega}^{(2)}_{lin}(ij)=-\frac{\bar{Z}}{2\pi}\left(\int_{\partial G_i}d\mathbf{r}\varphi_j+\int_{\partial G_j}d\mathbf{r}\varphi_i\right), \tag{13}$$

whereas the three-body terms (and higher) vanish. Triple forces can therefore not be calculated using linear theory and the superposition principle. This is not meant to imply that linear theory cannot be used to calculate triple forces in principle: one can, of course, linearize the PB equation of Eq. (9) and solve the full boundary value problem. The solution, satisfying all boundary conditions in Eq. (9), can deviate from the potential obtained from superposing one-colloid potentials, particularly if the colloidal spheres are large, the relative distances between them small, and the size of the double-layers involved comparable to the colloid dimension. This in principle should lead to three-body interactions. However, the region in parameter space where linearization is justifiable, but the superposition principle not, seems to be rather small. In almost all our calculations, we found that if the condition for the linearization of the problem was fullfilled, i.e., if the potential Φ on the colloidal surface was below unity, three-body effects completely disappeared. In other words, the nonlinearity of the PB problem is essential for the appearance of three-body interactions.

After this motivation to study the nonlinear PB problem, let us focus on the numerical methods and results. The strategy is to first compute $\bar{\Omega}_1$, for a given set of $(\bar{\kappa},\bar{Z})$, by solving the PB equation in the presence of a single colloid, and inserting the resulting solution $\Phi(\mathbf{r})$ into Eq. (10). This needs to be done only once, for a given set $(\bar{\kappa},\bar{Z})$. In principle we could then calculate $\bar{\Omega}_2(r_{12})$ for a set of distances r_{12} by solving the PB equation in the geometry of two colloids, and determine the pair interaction $\bar{\Omega}^{(2)}(r_{12})$ using Eq. (7). Along the same lines the three-body potential would follow from the solution of the PB equation in the geometry of three colloidal particles, together with Eq. (8). In practice, however, we find a larger numerical accuracy when the pair interactions $\bar{\Omega}^{(2)}(ij)$ of all three pairs of a triplet are calculated anew, for each triplet under investigation. This implies that we carry out, for a given configuration of three colloids, three two-body calculations to obtain $\bar{\Omega}^{(2)}(ij)$ for all three pairs, and one three-body calculation to determine $\bar{\Omega}_3$ and hence $\bar{\Omega}^{(3)}$. Varying some colloid-colloid distances in the triplet, each time going through the cycle just described, we end up with $\bar{\Omega}^{(3)}$ as a function of the three distances r_{12}, r_{13}, and r_{23}. The computational effort can be reduced if the sequence of configurations are chosen such that some of the pair interactions do not change or if the configurations are symmetric so that two or all three pair potentials are identical by symmetry.

To solve the PB-boundary value problem, Eq. (9), we use the finite element method [29]. An advantage of this numerical scheme is that one can locally vary the mesh size of the grid so as to improve the accuracy of the calculation in high-

gradient regions, for example, close to the particle surfaces. The initial task is to mesh the geometry, for which we use the program "Netgen" [30]. The grid thus generated is very fine on the colloidal surfaces and becomes smoothly coarser with increasing distance from the surface. Typically the colloidal surface is meshed by 7500 grid points, and a typical number for the total number of grid points is 2×10^5 for a relative accuracy of $\overline{\Omega}$ of 10^{-4}. For solving the differential equation on this grid we use the program package DIFFPACK [29]. Starting from a first guess of the solution one can use a built-in DIFFPACK procedure to further refine the grid, using the local information of an error estimation procedure. This involves the value of the solution over an element, its first derivative, and the volume of the element. This can be done iteratively. The original grid usually needs several refinements before the solution reaches sufficient overall accuracy.

Having solved $\Phi(\mathbf{r})$ on a grid from the nonlinear PB equation, we compute the grand potential using Eq. (10). Alternatively, one can directly calculate forces by integrating the stress tensor [which can also be written in terms of $\Phi(\mathbf{r})$] over a surface enclosing the particle of interest [31]. This alternative route offers a convenient way to check not only the whole implementation, but also the achieved accuracy, by comparing the forces between two colloids obtained from the stress-tensor procedure with the derivative of the pair potential calculated from Eq. (10). Another check was performed by comparing the numerically determined pair interaction with the DLVO potential, which should be valid in the linear regime of low *Z*. At low enough colloidal charge, both potentials and forces show virtually no deviation from the predictions of linear theory. However, for a given grid the potential obtained from Eq. (10) was more accurate than the forces calculated via the stress-tensor procedure. In other words, to calculate the force to the same accuracy as the potential one needs grids that must be considerably finer, thus requiring a much longer computation time. For most of our calculations, we therefore restricted ourselves to calculations of the grand potential only. For each set of parameters $(\overline{\kappa}^{-1},\overline{Z})$ we optimized the number of refinement steps with respect to both the desired accuracy and a reasonable computation time. We also checked for errors due to the finite size of our system.

B. Numerical results

Consistent with a mathematical proof [32], we find that the effective pair interaction $\overline{\Omega}^{(2)}(r_{12})$ is purely repulsive for any of the investigated values of $\overline{\kappa}$ and $\overline{Z}$. By contrast, we find that the triplet potential $\overline{\Omega}^{(3)}(r_{12},r_{13},r_{23})$ is purely attractive in all cases. A first illustration of the purely attractive nature of the three-body interactions is shown in Fig. 2 for coaxial geometries of the three particles, for the parameters $\overline{\kappa}^{-1}=6.25$, $\overline{Z}=6.75$. The symmetry of the coaxial geometry is such that $\overline{\Omega}^{(3)}$ only depends on the distance r_{12} between the left and the center sphere and the distance r_{23} between the center and the right sphere. Figure 2 shows the r_{23} dependence of $\overline{\Omega}^{(3)}$ for four different values of r_{12}. We observe that the three-body potential is indeed attractive in the coaxial geometry, and the more so the smaller the distances r_{12} and r_{23}. In order to compare the magnitude of $\overline{\Omega}^{(3)}$ with that of the pair interactions $\overline{\Omega}^{(2)}$, we plot in Fig. 3 the ratio $-\overline{\Omega}^{(3)}(123)/\overline{\Omega}^{(2)}(13)$ as obtained in the coaxial geometry, as a function of r_{23}, again for the four different values of r_{12}. One concludes from Fig. 3 that the three-body potential equals a considerable fraction of the negative of the pair interaction between the two outer particles, ranging from at least 40% at large r_{12} and r_{23} up to 90% at $r_{12},r_{23}\simeq\sigma$. This means that the middle colloid essentially shields the two outer ones from each other, indicative of strong three-body interactions in the coaxial geometry. This implies that the triplet interactions in the parallel plate geometry, as discussed in the Introduction, have indeed a direct analog in the geometry of spheres. The screening by the central sphere is not as perfect as by the central plate, but we deem the phenomenon identical.

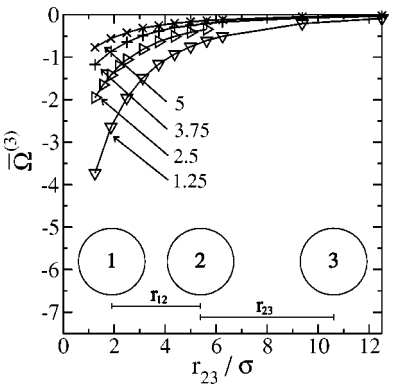

FIG. 2. Scaled effective three-body interaction $\overline{\Omega}^{(3)}=\beta\Omega^{(3)}\lambda_B/\sigma$ (see text) of three colloids, in the collinear geometry indicated in the graph, as a function of the separation r_{23} between the central and right-most colloidal particle. The curves are labeled by the value r_{12}/σ; the scaled screening length and charge are, respectively, $\overline{\kappa}^{-1}=6.25$ and $\overline{Z}=6.75$ for all curves. The three-body interaction is seen to be attractive.

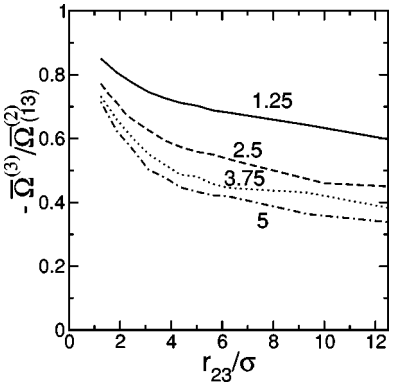

FIG. 3. Ratio $-\overline{\Omega}^{(3)}(123)/\overline{\Omega}^{(2)}(13)$ of the collinear three-body potentials (shown in Fig. 2) and the negative of the pair interaction $\overline{\Omega}^{(2)}(13)$ of the two outer spheres (labeled 1 and 3 as in Fig. 2). In the case of perfect shielding of the two outer particles by the central one, this ratio would take the value unity. The curves are labeled as in Fig. 2.

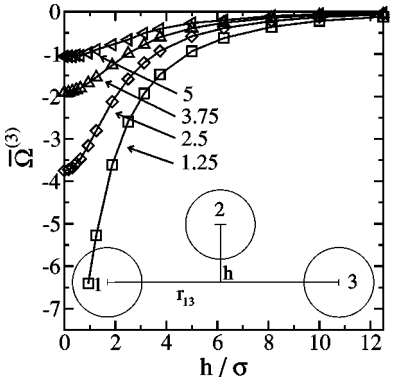

FIG. 4. Scaled effective three-body interaction $\overline{\Omega}^{(3)} = \beta\Omega^{(3)}\lambda_B/\sigma$ of three colloids in the midplane geometry, as a function of the distance h of the central colloid "2" from the axis between the two outer particles "1" and "3." Parameters are as in Fig. 2. The curves are labeled by the value r_{13}/σ.

We also calculated $\overline{\Omega}^{(3)}$ in two other geometries. In Figs. 4 and 5 we show results for the so-called "midplane" geometry and the equilateral triangle, respectively, again for $\overline{\kappa}^{-1} = 6.25$ and $\overline{Z} = 6.75$. In the midplane geometry the colloid labeled "2" is located in the midplane of the two outer colloids 1 and 3, shifted a distance h from the axis that connects the two outer ones. This implies that the case $h=0$ is a coaxial geometry, with $r_{12}=r_{23}=2r_{13}$, but by increasing h the central sphere is moved away perpendicular to the axis. Figure 4 shows $\overline{\Omega}^{(3)}$ as a function of h, for several separations r_{13} of the two outer spheres. Note that the minimal value of h for the curve with $r_{13}/\sigma = 1.25$ is set by the hard-sphere constraint, i.e., it corresponds to a 1-2 and 2-3 contact. The figure shows that $\overline{\Omega}^{(3)}$ is negative, and more so for smaller h and r_{13}, and hence represents attractive three-body interactions. The shielding of the two outer particles by the central one becomes less efficient for increasing h, as expected, but its effect dies down to zero only for a fairly large h of the order of a few σ. In other words, one does not require a strict colinear geometry to obtain a considerable shielding of the pairwise 13 interaction by colloid 2. At sufficiently large h we find that $\overline{\Omega}^{(3)} \to 0$ for any r_{13}, showing

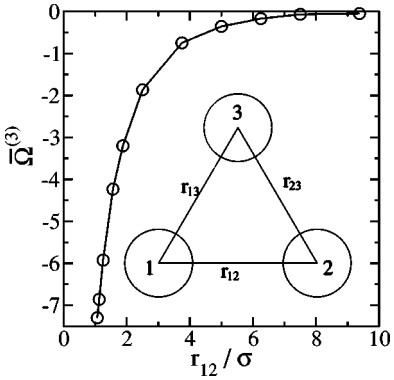

FIG. 5. Scaled effective three-body interaction $\overline{\Omega}^{(3)} = \beta\Omega^{(3)}\lambda_B/\sigma$ of three colloids in the equilateral triangle geometry, with $r_{12}=r_{23}=r_{13}$, as a function of r_{12}. Parameters are as in Fig. 2.

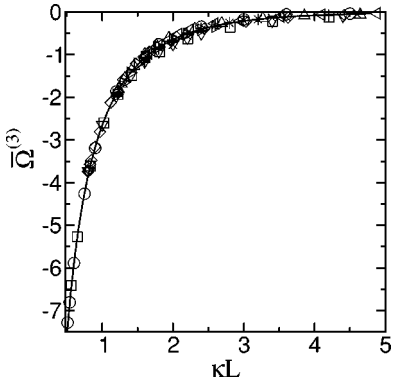

FIG. 6. The three-body potentials of Figs. 2, 4, and 5, plotted as a function of $L = r_{12}+r_{23}+r_{13}$. Circle symbols refer to the potentials calculated in the triangle configuration, squares to the potentials from the mid-plane configuration, and diamonds to those obtained in the axial configuration. The curve is a Yukawa function fitted to the data.

that pairwise additivity is restored when one of the three particles is far from the other two. This picture is confirmed by Fig. 5, where $\overline{\Omega}^{(3)}(r_{12})$ is plotted for the equilateral triangle geometry, with $r_{12}=r_{23}=r_{13}$. This configuration is the one where all three particles can touch each other. This configuration, with $r_{12}=\sigma$, gives the strongest, most negative $\overline{\Omega}^{(3)}$. For increasing sidelength of the triangle the triplet interaction decays to zero. Hence, $\overline{\Omega}^{(3)}$ represents attractive triplet interactions in the triangular geometry as well.

On the basis of Figs. 2, 4, and 5, which we consider a representative subset of all possible geometries of three particles, it is tempting to conclude that the triplet interaction is attractive for any geometry of three particles. This conclusion is confirmed by Fig. 6, which we deem the most important finding of the present study. In this figure we show *all* the triplet interactions of Figs. 2, 4, and 5, i.e., nine curves in total since all variations of the distances are considered, as a function of the summed distances

$$L = r_{12}+r_{13}+r_{23}. \tag{14}$$

The surprising result is that all data collapse onto one master curve that can be fitted remarkably well by a Yukawa function,

$$\overline{\Omega}^{(3)}(L) = -A^{(3)}\sigma\frac{e^{-\gamma L}}{L}, \tag{15}$$

with a decay parameter γ and an amplitude $A^{(3)}$. The full curve in Fig. 6 is the result of such a fit. Figure 6 indicates that the three-body potential depends, effectively, on the single distance L, rather than on the three distances r_{12}, r_{13}, and r_{23} separately. At this stage we have no satisfactory explanation for this observation. It implies that, in some sense, many of the details of the configuration are irrelevant for $\overline{\Omega}^{(3)}$.

We found this interesting property of three-body potentials for almost all combinations of $\overline{\kappa}^{-1}$ and $\overline{Z}$ investigated (for the region in parameter space studied in this work, see

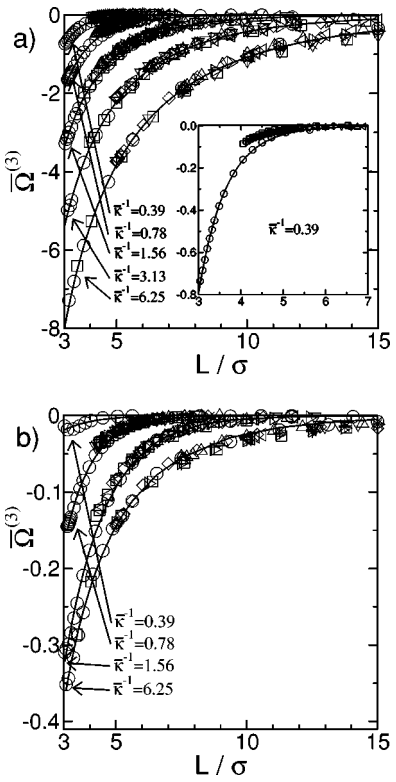

FIG. 7. Three-body potentials as a function of $L=r_{12}+r_{23}+r_{13}$, for various values of the parameter $\overline{\kappa}^{-1}$, in (a) for $\overline{Z}=6.75$ and in (b) for $\overline{Z}=1.8$. The inset figure shows a blowup of the results of the ($\overline{Z}=6.75$, $\overline{\kappa}^{-1}=0.39$) calculation in (a). The symbols refer to three-body potentials in different configurations [triangle, midplane, and axial configurations, same symbols as in Fig. (3)], the solid lines are fits of the data to the potential in Eq. (15).

Fig. 1). Figure 7 shows a few examples. For each pair of parameters $(\overline{\kappa}^{-1},\overline{Z})$, we first calculated the three-body interaction in all three configurations depicted and discussed above, i.e., the collinear, the midplane, and the triangle geometry. The resulting $\overline{\Omega}^{(3)}$ was then plotted as a function of L, and fitted to the potential given in Eq. (15); the fits are also shown in Fig. 7 as the full curves. The data collapse on a master curve is seen to hold, essentially, for all parameters $(\overline{\kappa}^{-1},\overline{Z})$. Figure 7 reveals that the three-body forces are attractive for all parameters investigated, with increasing strength for increasing values of $\overline{\kappa}^{-1}$. In the limit of very small values of $\overline{\kappa}^{-1}$, on the other hand, three-body effects disappear. A simple estimate for the minimal $\overline{\kappa}^{-1}$ required for nonvanishing triplet interactions can be given by considering three touching colloids in the equilateral triangle geometry—this is the situation where we expect, if existent, the strongest three-body interactions. Given that triplet interactions are due to an overlap of three double layers, each extending to a distance of order κ^{-1} from the colloidal surface, one can argue that triplet interactions exist when $\kappa^{-1}>\xi$, where ξ is the (smallest) distance from the center-of-mass position of the three colloids to the three colloidal surfaces. Elementary geometry yields $\xi/\sigma=1/\sqrt{3}-1/2\simeq 0.08$, and hence we expect the crossover to vanishing triplet interactions for $\overline{\kappa}^{-1}\simeq 0.08$. Note that this is an upper bound, in the sense that the touching triangle geometry is optimal for strong triplet interactions; other geometries require $\overline{\kappa}^{-1}>0.08$ for nonvanishing triplet interactions, consistent with our numerical findings shown in Fig. 7.

A comparison of Figs. 7(a) and 7(b) also reveals that $\overline{\Omega}^{(3)}$ is more than ten times larger for $\overline{Z}=6.75$ than for $\overline{Z}=1.8$. If one further reduces $\overline{Z}$, three-body potentials will eventually completely disappear. This is roughly the case when the electrostatic potential Φ becomes 1 at the colloidal surface, which is exactly the point where linear theory starts to become applicable. This again shows that three-body effects are a phenomenon of nonlinear theory.

In the triangle configuration L satisfies $L\geqslant 3\sigma$, where the minimal value $L=3\sigma$ obtains in the touching geometry. In all other configurations the minimum value for L is larger than 3σ. Therefore, the data for small values of L stem solely from the triangle configuration. For large values of $\overline{\kappa}^{-1}$ this is inconsequential, but this is relevant when $\overline{\kappa}^{-1}$ is so small that the triplet interaction decays to zero over one particle radius only. For a significant range of L we then only obtain data from the triangle configuration. This is actually the case for $\overline{\kappa}^{-1}=0.39$ as shown in the inset of Fig. 7(a). This inset also reveals that the data collapse is not exact. The deviation is systematic in that the triangle configuration, for fixed L, gives a stronger three-body interaction than the other configurations. However, we feel that this detail should not conceal the fact that the data collapse is remarkably accurate for the larger values of $\overline{\kappa}^{-1}$. Though unexplained, this property is of invaluable use in practical terms. For instance, a three-body interaction that depends on L only can be easily used in simulations. It is also helpful if one wishes to estimate the strength of three-body forces in a given system, as only calculations in, e.g., the triangle geometry need to be performed [recall that with the parametrization $(\overline{Z},\overline{\kappa})$ we treat the problem as generally as possible]. For these reasons we present the fit parameters $A^{(3)}$ and γ, based on Eq. (15), in Table I. We also give the prefactors $A^{(2)}$ for the calculated pair potentials $\overline{\Omega}^{(2)}$ (not shown here), fitted to

$$\overline{\Omega}^{(2)}(r)=A^{(2)}\sigma\frac{\exp[-\kappa r]}{r}. \tag{16}$$

Initially we also introduced the screening constant as a fit parameter for $\overline{\Omega}^{(2)}$, but we found it—to a very good approximation—equal to κ in all cases. The fits are of good quality, not only for long, but also for short distances.

C. Notes on the interaction range and on four-body interactions

If the range of $\overline{\Omega}^{(3)}$ is sufficiently large, then even fairly weak three-body interactions are thermodynamically relevant, since they lower the total interaction energy of a colloidal configuration. Here we briefly discuss some simple ideas to illustrate the effect qualitatively. Let us consider the energy per colloid, u, due to the effective interactions with other colloids. Due to the separation of the effective interac-

TABLE I. Parameters for three-body and two-body potentials in Eqs. (15) and (16) for various values of $(\overline{\kappa}^{-1},\overline{Z})$.

		$\overline{\kappa}^{-1}$						
$\overline{Z}$		0.39	0.5	0.78	1	1.56	3.13	6.25
9.00	$A^{(3)}$	1.3×10^{2}						
	$(\gamma\sigma)^{-1}$	0.80						
	$A^{(2)}$	3.5×10^{1}						
6.75	$A^{(3)}$	9.7×10^{1}		3.7×10^{1}		2.7×10^{1}	3.0×10^{1}	3.4×10^{1}
	$(\gamma\sigma)^{-1}$	0.80		1.6		3.0	5.0	8.5
	$A^{(2)}$	4.0×10^{1}		1.6×10^{1}		1.2×10^{1}	1.3×10^{1}	1.5×10^{1}
4.50	$A^{(3)}$	5.3×10^{1}						
	$(\gamma\sigma)^{-1}$	0.80						
	$A^{(2)}$	2.7×10^{1}						
3.38	$A^{(3)}$	5.3×10^{1}	3.5×10^{1}					
	$(\gamma\sigma)^{-1}$	0.75	1.0					
	$A^{(2)}$	1.9×10^{1}	1.3×10^{1}					
2.25	$A^{(3)}$	2.5×10^{1}						
	$(\gamma\sigma)^{-1}$	0.65						
	$A^{(2)}$	1.1×10^{1}						
1.80	$A^{(3)}$	9.0×10^{0}	6.0×10^{0}	4.1×10^{0}		3.2×10^{0}	2.9×10^{0}	2.2×10^{0}
	$(\gamma\sigma)^{-1}$	0.70	1.0	1.5		2.6	3.7	4.5
	$A^{(2)}$	6.5×10^{0}	5.1×10^{0}	3.5×10^{0}		2.9×10^{0}	2.9×10^{0}	3.0×10^{0}
1.35	$A^{(3)}$			1.6×10^{0}	1.7×10^{0}	9.7×10^{-1}	8.7×10^{-1}	
	$(\gamma\sigma)^{-1}$			1.4	1.6	2.9	4.5	
	$A^{(2)}$			2.2×10^{0}	2.0×10^{0}	1.8×10^{0}	1.8×10^{0}	
0.900	$A^{(3)}$			1.2×10^{-1}	2.6×10^{-1}	1.8×10^{-1}	1.4×10^{-1}	
	$(\gamma\sigma)^{-1}$			1.7	1.7	2.9	4.1	
	$A^{(2)}$			1.0×10^{0}	9.3×10^{-1}	8.4×10^{-1}	8.0×10^{-1}	
0.675	$A^{(3)}$				3.8×10^{-2}	5.7×10^{-2}	2.6×10^{-2}	1.4×10^{-2}
	$(\gamma\sigma)^{-1}$				1.9	2.6	6.5	7.5
	$A^{(2)}$	3.7×10^{0}			5.4×10^{-1}	5.0×10^{-1}	4.6×10^{-1}	4.5×10^{-1}
0.450	$A^{(3)}$							2.0×10^{-3}
	$(\gamma\sigma)^{-1}$							9.5
	$A^{(2)}$				2.5×10^{-1}	6.5×10^{-1}		2.0×10^{-1}
0.338	$A^{(3)}$							5.2×10^{-4}
	$(\gamma\sigma)^{-1}$							6
	$A^{(2)}$				1.35×10^{-1}			1.1×10^{-1}

tions into pair-, triplet-, and more-body contributions, we can write $u=u_2+u_3+\cdots$, with u_k the contribution to u from the k-body interactions $\Omega^{(k)}$. In a van der Waals-like mean-field picture [33], one estimates that $u_k\simeq n_k\omega_k/k!$, with ω_k the typical strength of $\Omega^{(k)}$ and n_k the number of k tuplets in the range of $\Omega^{(k)}$. At total density ρ and range ξ—which we take the same here for all k for simplicity, and this is supported by our data—this yields $n_2=\rho\xi^3$ and $n_3=(\rho\xi^3)^2$, and hence $u_3/u_2=(\omega_3/\omega_2)\rho\xi^3$ is obtained for the ratio of three-body to two-body interaction energy. At great interaction ranges even small three-body interactions can be of importance to the overall interaction energy. Our data show that ω_3/ω_2 is, typically, of order unity, and that $\xi\simeq\kappa^{-1}$. Hence, the triplet interactions should be considered relevant when $\rho\kappa^{-3}\simeq\eta\overline{\kappa}^{-3}$ is of order unity, where $\eta=(\pi/6)\rho\sigma^3$ is the colloidal packing fraction.

Another point of interest is the next order term, the four-body interaction $\Omega^{(4)}$, which of course also becomes relevant if the range of the interactions increases. The main problem is that it depends on six (combinations of) coordinates—recall that $\Omega^{(3)}$ depends on three coordinates, and that its study was only feasible practically because of the empirical observation that the dependence on all r_{ij} could be reduced to a single L dependence. For these computational reasons we restricted attention to only two classes of configurations, and to a very limited set of $(\overline{Z},\overline{\kappa}^{-1})$. The first class of configuration is the collinear one, where the four colloids are perfectly aligned on a single axis, and the second one is the tetraeder configuration, where the four colloids form the corners of a symmetric tetraeder. On the basis of the four-body interactions of parallel plates [28], discussed in the introduction, we expected $\Omega^{(4)}$ to represent repulsive interactions. To our surprise, however, we find that $\Omega^{(4)}$ is *attractive* for all configurations of four spheres that we considered here. We have, moreover, some evidence that $\Omega^{(4)}$ can also be represented realistically as a function of the summed distances

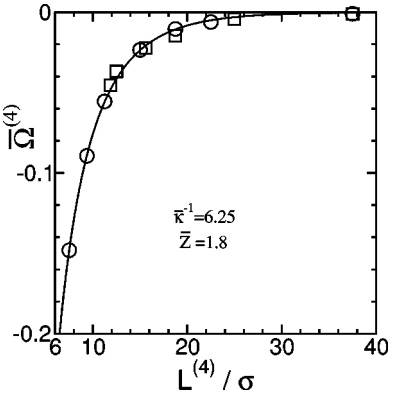

FIG. 8. Scaled effective four-body interaction $\bar{\Omega}^{(4)}$ of four colloids, in the colinear and tetraedral geometry, plotted as a function of $L^{(4)}=\Sigma_{i<j}^{4} r_{ij}$.

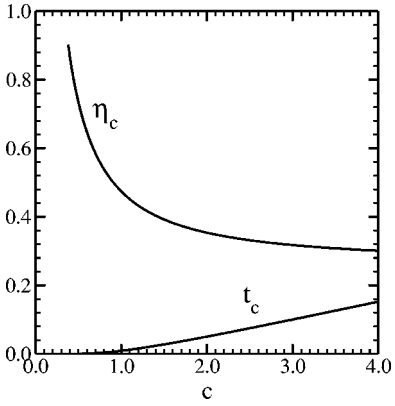

FIG. 9. Critical packing fraction, η_c, and critical "temperature" t_c as a function of the relative strength c of the triplet interactions, see text.

involved, i.e., $\Omega^{(4)}(\{r_{ij}\})=\Omega^{(4)}(L^{(4)})$, with $L^{(4)}=\Sigma_{i<j}^{4} r_{ij}$. The data onto which this reduction is based is rather limited, however. As an example, we show $\bar{\Omega}^{(4)}$ as a function of $L^{(4)}$ in Fig. 8, for $\bar{\kappa}^{-1}=6.25$ and $\bar{Z}=1.8$. The typical magnitude of the four-body attractions is found to be much weaker than any of the corresponding three-body attractions. Note, however, that a direct comparison of the numerical value of $\Omega^{(3)}$ and $\Omega^{(4)}$ should be carried out with care: the contact value for the triplet interactions takes place at $L^{(3)}=L=3\sigma$, and for the four-body interactions at $L^{(4)}=6\sigma$, so it should come as no surprise that the four-body potential has a lower numerical value. A better comparison would be based on the integrated strengths ω_3 and ω_4, discussed above. We did not pursue this here for technical reasons.

IV. GAS-LIQUID COEXISTENCE?

In the final section of this paper we wish to roughly estimate whether or not the cohesive energy hidden in the triplet interactions can possibly drive gas-liquid coexistence. We do this using the simplest possible extension of the van der Waals theory for gas-liquid coexistence; more elaborate descriptions are straightforward to formulate but not considered here. We take the hard-sphere fluid, with diameter σ and number density ρ, as the reference fluid, and consider the pairwise repulsions and the triplet attractions calculated in this paper as weak perturbations—this is a strong assumption that can be relaxed at the expense of more involved calculations. Within a mean-field picture, where the pair correlations of the hard-sphere fluid are assumed to be unity for $r>\sigma$, the Helmholtz free energy F of the effective one-component system in a bulk volume V can be written, in dimensionless form $f=Fv_0/VkT$, as the sum of hard-sphere, pair, and triplet contributions, viz.,

$$f=f^{(\mathrm{HS})}+a\,\eta^2-b\,\eta^3, \tag{17}$$

where $v_0=(\pi/6)\sigma^3$ is the volume of a colloidal sphere, and where $\eta=\rho v_0$ is the packing fraction. Here $f^{(\mathrm{HS})}$ is the hard-sphere free energy, for which we take the Carnahan-Starling form

$$f^{(\mathrm{HS})}=\eta\left(\ln\eta-1+\frac{4\eta-3\eta^2}{(1-\eta)^2}\right). \tag{18}$$

The coefficients a and b are the integrated strengths of the pair and triplet interactions in units of kT, viz.,

$$a=\frac{1}{2v_0}\int d\mathbf{r}\beta\Omega^{(2)}(\mathbf{r}) \tag{19}$$

$$b=-\frac{1}{6v_0^2}\int d\mathbf{r}_{12}\int d\mathbf{r}_{13}\beta\Omega^{(3)}(\mathbf{r}_{12},\mathbf{r}_{13}). \tag{20}$$

Note that a and b are dimensionless, and that their signs are chosen such that both are positive here. The standard van der Waals-like theories for simple fluids, where the pair-interactions are attractive beyond the hard-sphere radius and where the triplet interactions are assumed to be nonexistent, are recovered by taking $a<0$ and $b=0$ in Eq. (17). The present description can also be seen as an extension to the ideas put forward by Sear in [33], where attractive triplet forces were considered without any long-range pair forces, i.e., where $a=0$ and $b>0$. The point here is that the cohesive energy is in the cubic (three-body) term, while the quadratic (two-body) term is a positive (repulsive) addition to the hard-sphere free energy.

The existence of a critical point can be inferred from Eq. (17) by solving for the conditions $f''=0$ and $f'''=0$, where a prime denotes a derivative with respect to η. These two conditions, which can easily be solved numerically, imply two constraints on the three parameters η, a, and b. In order to make the connection with the original van der Waals theory as transparent as possible, we define a (dimensionless) temperature variable as $t=1/a$, and a parameter $c=b/a$ that denotes the relative strength of triplet interactions. In Fig. 9 we plot the critical packing fraction η_c and the critical temperature t_c as a function of c. With increasing c, i.e., with increasing strength and/or range of the triplet attractions compared to the pairwise repulsions, we see that t_c increases and η_c decreases. The question now is, in which regime should we position the parameters a and b, and hence t and c, for the

charged colloids of interest? If we take the pair potential of the Yukawa form of Eq. (16), which turned out to be an accurate representation, then $t=1/a$ follows directly from Eq. (19),

$$t=\frac{\lambda_B}{\sigma}\frac{\overline{\kappa}^2\exp(\overline{\kappa})}{12A^{(2)}(1+\overline{\kappa})}. \tag{21}$$

In typical colloidal systems λ_B/σ ranges between 10^{-2} and 10^{-3} ($\lambda_B=0.7$ nm for water, σ typically between 100 and 1000 nm), so that using the values for $A^{(2)}$ from our fits (Table I) for $\overline{Z}=6.75$ we find temperatures between $t=10^{-8}$ for $\overline{\kappa}=0.39$ and $t=10^{-3}$ for $\overline{\kappa}=6.25$. Note that for the calculation of a temperature our scaled quantities are not sufficient, but that specific values for the ratio λ_B/σ are now required.

Comparing these typical temperatures t with the numerical values for t_c in Fig. 9, one observes that $t<t_c$ (or even $t\ll t_c$) in the regime $c>1$, say. In other words, in the regime $c>1$, a typical suspension is predicted to be subcritical, which implies that the triplet attractions are strong enough to drive a typical suspension into gas-liquid equilibrium at high enough η. The next question is, therefore, which values of c we find from our calculations of $\overline{\Omega}^{(2)}$ and $\overline{\Omega}^{(3)}$. The answer to this question is greatly simplified due to the data collapse of the triplet interactions onto a master curve. Since $\overline{\Omega}^{(3)}$ only depends on $L=r_{12}+r_{13}+r_{23}$ it follows that its equipotential surface for fixed $r_{12}=r$ (i.e., particle 1 and 2 are fixed) is an ellipsoid with long axis $L-r$ and short axis $\sqrt{L^2-2Lr}$, and focal points on the positions of particles 1 and 2. The surface area $S(r,L)$ of this ellipsoid follows from elementary geometry, and can be used to simplify Eq. (20) as

$$b=-\frac{1}{6v_0^2}\int_\sigma^\infty dr 4\pi r^2\int_{2r}^\infty dL S(r,L)\beta\Omega^{(3)}(L). \tag{22}$$

Using the fitted form of Eq. (15) one easily evaluates b numerically. Of course the evaluation of a is also straightforward, e.g., from the fit of Eq. (16), and hence c is deduced from the calculations of the pair and triplet interactions. In Fig. 10 we show all parameter combinations $(\overline{\kappa}^{-1},\overline{Z})$ that we considered in this study once again, cf. Fig. 1, but here we distinguish between points with $c<1$ (indicated by ○) and points with $c>1$ (indicated by × and diamond symbols). The full curve in Fig. 10 is an estimate to the line $c=1$, which we propose to be a reasonable demarcation between the subcritical and supercritical regimes—at least on the basis of the van der Waals theory discussed here. In order to check again if the systems in the $c>1$ region have a temperature $t<t_c$ we have calculated the temperatures for all state points using the values in Table I in Eq. (21) (assuming $\lambda_B/\sigma=10^{-2}$) and compared them to t_c at that specific c. Indeed, except for three points (filled diamonds in Fig. 10), this condition is always fullfilled. The graph reveals, quite reasonably, that high colloidal charges and low-salt conditions facilitate gas-liquid coexistence. We stress, however,

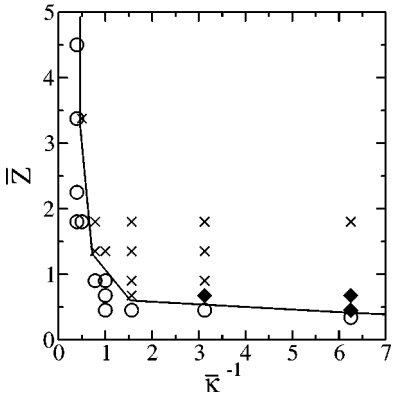

FIG. 10. Parameters investigated in this work, with × symbols for parameters such that $c>1$ and $t<t_c$, and ○ for $c<1$ (see text). The filled diamonds correspond to systems for which $c>1$, but $t>t_c$ assuming $\lambda_B/\sigma=10^{-2}$. The curve is an estimate for the line $c=1$, above which a gas-liquid coexistence is to be expected on the basis of the van der Waals–like theory.

that our location of this line is highly approximate. Perhaps the most important result in this respect is that there *is* a demarcation line in the $(\overline{\kappa}^{-1},\overline{Z})$ plane. Given that the triplet interactions for any combination of Debye length κ^{-1}, colloidal charge Z, Bjerrum length λ_B, and colloidal diameter σ can be characterized by $\overline{\kappa}^{-1}$ and $\overline{Z}$, this should be appreciated as a substantial result.

We did not analyze whether or not the critical point and the gas-liquid coexistence are stable with respect to the freezing transition. The results of Ref. [33] suggest that the range of stability of the liquid phase (i.e., the ratio of the critical temperature and the triple-point temperature) shrinks considerably when the cohesion energy is provided by triplet instead of pair interactions. Because of the additional presence of pairwise repulsion in the present case, we expect the liquid phase to be stable in an even smaller pocket of the phase diagram than is the case in Ref. [33]. As a consequence, the triplet attractions are most likely to drive a gas-solid instead of a gas-liquid coexistence. The key point is, however, that a dilute suspension of highly charged colloids is predicted to coexist, at low enough salt concentrations, with a much denser phase, either a liquid or a crystal.

V. CONCLUDING REMARKS

We have presented numerical calculations of the pair and triplet potential of charged colloidal particles in an electrolyte solution within Poisson-Boltzmann theory. The pair interaction is found to be repulsive in all cases, consistent with the traditional DLVO theory. By contrast, the triplet potential is attractive in all geometries considered, and thus provides some (effective) cohesion to the suspension. The physical mechanism is, essentially, that the presence of a colloidal particle in between two others largely shields the direct (repulsive) pair interaction between the latter two. In other words, the triplet interaction describes, to the lowest order, the screening by the macroions.

Our results are consistent with the results of Refs. [26,27],

where the equilateral triangle configuration of charged colloids was found to generate an attractive triplet force that represents a substantial correction to the repulsive pair forces. However, our results seem to be inconsistent with those of Ref. [34], where a free-energy functional is minimized with respect to the counterion density profile (there are no coions) with the Car-Parinello scheme. Even though the colloidal charge and diameter studied in Ref. [34] are similar to the regime of our study, there is no evidence for triplet forces, neither attractive nor repulsive, in Ref. [34]. Important differences between the present study and that of Ref. [34] are the periodic box and the cubic grid of Ref. [34] compared to our single box and adaptive grid. Other differences include the absence of added salt in Ref. [34], and the inclusion of a correlation term (at the OCP level) in the functional of Ref. [34]. Given the low microion density we argue, based on Ref. [35], that the inclusion of some correlations should not make a quantitative difference. The absence of added salt, i.e., the absence of a fixed Debye length could, on the other hand, be an important source of the different conclusions, since this may induce some (unwanted) system size dependence to the distribution of the ions and hence to the screening. We leave this as an unsettled issue here.

We argued that the triplet attractions can be interpreted in terms of screening by macroions (and the counterions that come with the macroions). Such a macroion screening effect has recently been observed in an experiment where the radial distribution function (RDF) of a two-dimensional colloidal system was measured at several colloid densities [36]. The RDFs thus obtained were inverted to give the effective colloid-colloid pair potentials. At relatively low densities the measured pair potentials were found to be of purely repulsive Yukawa form. By contrast, at higher densities substantial deviations from the Yukawa potential were observed at distances comparable to the mean colloid-colloid distance $D=\rho^{-1/2}$. This suggests that the interaction of two colloids at a distance $r>D$ is simply blocked by a third macroion, which is located, on average, at D and thus somewhere in between the two interacting colloids under consideration. The present study demonstrates that this blocking is very effective indeed, see Fig. 3. Having in mind that the three-body potentials calculated in the present work are negative, it is clear that an inversion procedure that only allows for pair potentials yields a density-dependent negative contribution to that pair interaction: in some sense the attractive three-body potential is ''projected'' into the space of pair-potentials. If the triplet attraction is strong enough such a projection may even cause density-dependent effective pair attractions, which one then easily interprets as ''like-charge attraction.''

While in Ref. [36] the screening length of the microions, $\overline{\kappa}^{-1}$, was relatively small ($\overline{\kappa}^{-1}=0.2$), we have found here that the strength of the three-body potentials increases with increasing $\overline{\kappa}^{-1}$ (and $\overline{Z}$). The triplet potential is found to be particularly strong if κ^{-1} is of the order or larger than the colloidal diameter σ, i.e., $\kappa\sigma<1$ or $\overline{\kappa}^{-1}>1$. For a typical colloidal diameter of $\sigma\simeq 100$ nm this corresponds, for water at room temperature as a solvent, to extremely low salt concentrations of the order of a few μM, i.e., the regime where recent experiments have revealed evidence, albeit sometimes controversial, for like-charge attractions and gas-liquid equilibrium. Our study strongly suggests that many-body interactions are the source of these alleged observations.

A very important result of our study is that the triplet interaction turns out to be a function of the summed distance $L=r_{12}+r_{13}+r_{23}$ between the three particles only. This empirical observation, for which we do not have a satisfactory explanation, is important as it greatly simplifies the representation of the triplet interactions, e.g., in terms of a limited number of fit parameters. In Table I we present the fit parameters based on Eq. (15) for all parameter sets $(\overline{\kappa}^{-1},\overline{Z})$ that we considered in this study. They may be useful for simulation purposes, e.g., to study the possibility of gas-liquid (or gas-solid) equilibrium beyond the van der Waals-like mean-field theory presented in the final section of this paper.

ACKNOWLEDGMENTS

We gratefully acknowledge fruitful discussions with Rudolf Klein and Alfons van Blaaderen, and the financial support from the DFG through SFB 513. This work is part of the research program of the ''Stichting voor Fundamenteel Onderzoek der Materie (FOM),'' which is financially supported by the ''Nederlandse Organisatie voor Wetenschappelijk Onderzoek (NWO).''

[1] B. Derjaguin and L. Landau, Acta Physicochim. URSS **14**, 633 (1941); E. J. W. Verwey and J. Th. G. Overbeek, *Theory of the Stability of Lyotropic Colloids* (Elsevier, Amsterdam, 1948).
[2] J.M. Victor and J.P. Hansen, Trans. Faraday Soc. **81**, 43 (1985).
[3] W.B. Russel, D.A. Saville, and W.R. Schowalter, *Colloidal Dispersions* (Cambridge University Press, Cambridge, 1989).
[4] K. Ito, H. Yoshida, and N. Ise, Science **263**, 66 (1994); B.V.R. Tata, E. Yamahara, P.V. Rajamani, and N. Ise, Phys. Rev. Lett. **78**, 2660 (1997).
[5] N. Ise, T. Obuko, M. Sugimura, K. Ito, and H.J. Nolte, J. Chem. Phys. **78**, 536 (1983); N. Ise and M.V. Smalley, Phys. Rev. B **50**, 16 722 (1994).
[6] A.E. Larsen and D.G. Grier, Nature (London) **385**, 230 (1997).
[7] B.V.R. Tata, M. Rajalakshmi, and A.K. Arora, Phys. Rev. Lett. **69**, 3778 (1992).
[8] T. Palberg and M. Würth, Phys. Rev. Lett. **72**, 786 (1994).
[9] L. Belloni, J. Phys.: Condens. Matter **12**, R549 (2000).
[10] M. Dijkstra, Curr. Opin. Colloid Interface Sci. **6**, 372 (2001).
[11] J.P. Hansen and H. Löwen, Annu. Rev. Phys. Chem. **51**, 209 (2000).
[12] M.J. Stevens and M.O. Robbins, Europhys. Lett. **12**, 81 (1990).
[13] O. Spalla and L. Belloni, Phys. Rev. Lett. **74**, 2515 (1995).
[14] J. Ray and G.S. Manning, Langmuir **10**, 2450 (1994).
[15] B.Y. Ha and A.J. Liu, Phys. Rev. Lett. **79**, 1289 (1997).

[16] R. Podgornik and V.A. Parsegian, Phys. Rev. Lett. **80**, 1560 (1998).
[17] Y. Levin, M.C. Barbosa, and M.N. Tamashiro, Europhys. Lett. **41**, 123 (1998); Y. Levin, Physica A **265**, 432 (1999); A. Diehl, M.C. Barbosa, and Y. Levin, Europhys. Lett. **53**, 86 (2001).
[18] R.R. Netz and H. Orland, Europhys. Lett. **45**, 726 (1999).
[19] E. Allahyarov, I. D'Amico, and H. Löwen, Phys. Rev. Lett. **81**, 1334 (1998).
[20] B. Beresford-Smith, D.Y.C. Chan, and D.J. Mitchell, J. Colloid Interface Sci. **105**, 215 (1985); D.Y.C. Chan, Phys. Rev. E **63**, 061806 (2001).
[21] R. van Roij and J.P. Hansen, Phys. Rev. Lett. **79**, 3082 (1997); R. van Roij, M. Dijkstra, and J.P. Hansen, Phys. Rev. E **59**, 2010 (1999); R. van Roij and R. Evans, J. Phys.: Condens. Matter **11**, 10 047 (1999); R. van Roij, *ibid.* **12**, A263 (2000).
[22] P.B. Warren, J. Chem. Phys. **112**, 4683 (2000).
[23] M.J. Grimson and M. Silbert, Mol. Phys. **74**, 397 (1991).
[24] H. Graf and H. Löwen, Phys. Rev. E **57**, 5744 (1998).
[25] H.H. von Grünberg, R. van Roij, and G. Klein, Europhys. Lett. **55**, 580 (2001).
[26] H. Löwen and E. Allahyarov, J. Phys.: Condens. Matter **10**, 4147 (1998).
[27] J.Z. Wu, D. Bratko, H.W. Blanch, and J.M. Prausnitz, J. Chem. Phys. **113**, 3360 (2000).
[28] R. van Roij (unpublished).
[29] H.P. Langtangen, *Computational Partial Differential Equations* (Springer, Berlin, 1999); Numerical Objects, http://www.nobjects.com/
[30] Joachim Schöberl, http://www.sfb013.uni-linz.ac. at/ joachim/ netgen/
[31] H.H. von Grünberg and E.C. Mbamala, J. Phys.: Condens. Matter **13**, 4801 (2001).
[32] J.C. Neu, Phys. Rev. Lett. **82**, 1072 (1999).
[33] R.P. Sear, Phys. Rev. E **61**, 651 (2000).
[34] R. Tehver, F. Ancilotto, F. Toigo, J. Koplik, and J.R. Banavar, Phys. Rev. E **59**, R1335 (1999).
[35] H. Löwen, J.P. Hansen, and P.A. Madden, J. Chem. Phys. **98**, 3275 (1993).
[36] M. Brunner, C. Bechinger, W. Strepp, V. Lobaskin, and H.H. von Grünberg (unpublished).